Pis'ma Red. **7**, 464 (1968) [JETP Lett. **7**, 360 (1968)].
[11]A. A. Rogachev, in *Proceedings of the Ninth International Conference on the Physics of Semiconductors*, Moscow, 1968 (Nauka, Leningrad, 1968), p. 407.
[12]A. S. Alekseev, V. S. Bagaev, T. I. Galkina, O. V. Gogolin, N. A. Penin, A. N. Semenov, and V. G. Stopachinskii, Zh. Eksp. Teor. Fiz. Pis'ma Red. **12**, 203 (1970) [JETP Lett. **12**, 140 (1970)].
[13]V. E. Pokrovskii and K. I. Svistunova, Zh. Eksp. Teor. Fiz. Pis'ma Red. **9**, 435 (1969) [JETP Lett. **9**, 261 (1969)].
[14]Y. Nishina, T. Nakanomyo, and T. Fukase, in *Tenth International Conference on the Physics of Semiconductors - Extended Abstracts, Cambridge, Mass. 1970* (U. S. AEC, Oak Ridge, Tenn., 1970), p. 163.
[15]U. Heim, O. Röder, and M. H. Pilkuhn, Solid State Commun. **7**, 1173 (1969); E. Göbel, H. J. Queisser, and M. H. Pilkuhn, Solid State Commun. **9**, 429 (1971).
[16]T. Goto and D. Langer, Phys. Rev. Lett. **27**, 1004 (1971); R. F. Leheny, R. E. Nahory, and K. L. Shaklee, Phys. Rev. Lett. **28**, 437 (1972).
[17]V. M. Asnin and A. A. Rogachev, Zh. Eksp. Teor. Fiz. Pis'ma Red. **9**, 415 (1969) [JETP Lett. **9**, 248 (1969)]; see C. Benoit à la Guillaume, M. Voos, and F. Salvan, Phys. Rev. B **5**, 3079 (1972) for a recent review.
[18]J. R. Haynes, Phys. Rev. Lett. **17**, 860 (1966).
[19]A. Mysyrowicz, J. B. Grun, R. Levy, A. Bivas, and S. Nikitine, Phys. Rev. Lett. **26A**, 615 (1968); R. S. Knox, S. Nikitine, and A. Mysyrowicz, Opt. Commun. **1**, 19 (1969); H. Souma, T. Goto, and M. Ueta, J. Phys. Soc. Jap. **29**, 697 (1970); J. B. Grun, S. Nikitine, A. Bivas, and R. Levy, J. Lumin. **1/2**, 241 (1970).
[20]H. Souma, T. Goto, and M. Ueta, J. Phys. Soc. Jap. **31**, 1285 (1971).
[21]C. I. Yu, T. Goto, and M. Ueta, J. Phys. Soc. Jap. **32**, 1671 (1972).
[22]S. Shionoya, H. Saito, E. Hanamura, and O. Akimoto, Solid State Commun. **12**, 223 (1973).
[23]R. L. Shaklee, R. F. Leheny, and R. E. Nahory, Phys. Rev. Lett. **26**, 888 (1971).
[24]R. R. Sharma, Phys. Rev. **170**, 770 (1968); R. K. Wehner, Solid State Commun. **7**, 457 (1969); J. Adamowski and S. Bednarck, Solid State Commun. **9**, 2037 (1971).
[25]O. Akimoto and E. Hanamura, Solid State Commun. **10**, 253 (1972); W.-T. Huang and U. Schröder, Phys. Lett. **38A**, 507 (1972).
[26]S. A. Moskalenko, Fiz. Tverd. Tela **4**, 276 (1962) [Sov. Phys.-Solid State **4**, 199 (1962)].
[27]R. C. Casella, J. Phys. Chem. Solids **24**, 19 (1963).
[28]I. K. Akopyan, E. F. Gross, and B. S. Razbirin, Zh. Eksp. Teor. Fiz. Pis'ma Red. **12**, 366 (1970) [JETP Lett. **12**, 251 (1970)].
[29]B. M. Ashkinadze, I. P. Kretsu, S. M. Ryvkin, and I. D. Yaroshetskii, Zh. Eksp. Teor. Fiz. **58**, 507 (1970) [Sov. Phys.-JETP **31**, 271 (1970)].
[30]R. Levy, J. B. Grun, H. Haken, and S. Nikitine, Solid State Commun. **10**, 915 (1972).
[31]L. V. Keldysh and A. N. Kozlov, Zh. Eksp. Teor. Fiz. **54**, 978 (1968) [Sov. Phys.-JETP **27**, 521 (1968)].
[32]V. A. Gergel, R. F. Kazarinov, and R. A. Suris, Zh. Eksp. Teor. Fiz. **53**, 544 (1967) [Sov. Phys.-JETP **26**, 354 (1968)].
[33]W. F. Brinkman, T. M. Rice, P. W. Anderson, and S. T. Chui, Phys. Rev. Lett. **28**, 961 (1972); E. Hanamura and M. Inoue, in Proceedings of the Eleventh International Conference on the Physics of Semiconductors, Warsaw, 1972 (unpublished).).
[34]K. L. Shaklee and R. F. Leheny, Appl. Phys. Lett. **18**, 475 (1971).
[35]J. Bille, H. Liebing, and P. Mengel, Phys. Status Solidi B **53**, 353 (1972).

PHYSICAL REVIEW B VOLUME 7, NUMBER 10 15 MAY 1973

Dispersion Curves and Elastic Constants of Graphite

Aziz A. Ahmadieh and Hamid A. Rafizadeh
Department of Materials Science and Engineering, Pahlavi University, Shiraz, Iran
(Received 28 June 1972)

Lattice vibrations of the hexagonal graphite crystal are analyzed using two-body carbon-carbon interaction potentials. The potential parameters are obtained from estimates of the long-wavelength frequencies of graphite and a knowledge of the nitrogen-nitrogen potential parameters. The dispersion relations along high-symmetry directions are calculated showing excellent agreement with the experimental observations along (00ξ). The elastic constants of graphite are also calculated and compared with the available experimental data. There is general agreement between the theoretical calculations and the experimental observations.

I. INTRODUCTION

The lattice dynamics of graphite have been discussed by several authors using few-parameter Born–von Karman models.[1–6] The unknown parameters of the models are fitted to the experimental data such as specific heat[7] and the measurements of phonon dispersion relations.[8] The graphite structure assumed in lattice-dynamical calculations corresponds to the hexagonal crystal structure where sheets of carbon atoms are stacked on one another and held by van der Waals forces. The forces in the sheets are due to the strong covalent forces. This structure is highly anisotropic in properties such as thermal expansion and elasticity.[7]

In this paper we intend to analyze the lattice vibrations of graphite in the hexagonal crystal structure. The lattice-dynamical model employed will be the usual Born–von Karman model in which significant interactions between carbon atoms are represented by finite-value force constants. However, our approach will be different from previous attempts in the use of analytical potentials for car-

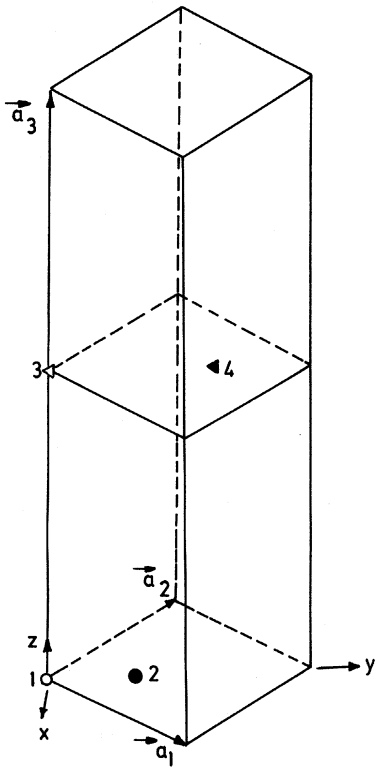

FIG. 1. Hexagonal primitive unit cell of graphite. Carbon atoms are shown by open and full circles and triangles.

bon-carbon interactions. This will result in a few-parameter model rather than a few-force-constant model of graphite. Two-body analytical potentials of interaction have been successfully used in the analysis of lattice dynamics of organic solids such as naphthalene and anthracene[9,10] and inorganic solids such as sodium azide.[11] With the two-body interaction potentials the properties of graphite are essentially predicted rather than fitted to the model parameters. This will be illustrated by the calculation of the dispersion relations and the elastic constants.

In Sec. II the structure of graphite and the significant carbon-carbon interactions are introduced and the dynamical matrix is calculated. The elements of the dynamical matrix are given in Appendix A. Although the number of unknown force constants is irrelevant when using two-body interaction potentials, the force constants are reduced in number for the sake of simplicity of the dynamical matrix elements. The reduction in number of these constants is made according to the proper symmetry reductions belonging to the point group of graphite crystals.

In Sec. III the information on the long-wavelength frequencies of benzene molecule and the nitrogen-nitrogen van der Waals interaction potential are used to arrive at reasonable estimates of the carbon-carbon potentials of interaction. In Sec. IV the dispersion relations and the structure factors along high-symmetry directions are calculated. Section V includes the calculation of the elastic constants and their comparison with the experimental data.[12] In Sec. VI the essential features of our work are summarized and some of the structural characteristics of graphite are discussed.

II. DYNAMICAL MATRIX OF GRAPHITE

The familiar structure of graphite consists of a hexagonal structure[13] in which the carbon atoms form covalently bonded planes which are stacked parallel to one another. Within the planes each carbon atom forms covalent sp^2 bonds with three other carbon atoms resulting in a hexagonal arrangement very similar to the structure of benzene ring. The hexagonal unit cell of graphite is shown in Fig. 1 with the direct lattice vectors

$$\begin{aligned}\vec{a}_1 &= \tfrac{1}{2}a\hat{x} + \tfrac{1}{2}\sqrt{3}\,a\hat{y}\,,\\ \vec{a}_2 &= -\tfrac{1}{2}a\hat{x} + \tfrac{1}{2}\sqrt{3}\,a\hat{y}\,,\\ \vec{a}_3 &= c\hat{z}\,,\end{aligned} \tag{1}$$

where $a = 2.456$ Å and $c = 6.696$ Å. The basis of this unit cell consists of four carbon atoms located at positions of 000, $\frac{1}{3}\frac{1}{3}0$, $00\frac{1}{2}$, $\frac{2}{3}\frac{2}{3}\frac{1}{2}$ and labeled as carbons 1, 2, 3, and 4, respectively. The notation $n_1n_2n_3$ refers to the position of carbon atoms in the unit cell given by $n_1\vec{a}_1 + n_2\vec{a}_2 + n_3\vec{a}_3$.

We will consider the neighbors of each of these atoms in two categories of the in-plane and out-of-plane interactions. For the in-plane interactions either (11), (22), (12), or (33), (44), (34) interactions are possible. For the out-of-plane interactions the possible interactions are (13), (14), and (23), (24). The in-plane neighbors of the carbon atom 1 are shown in Fig. 2(a). There are six (11) interactions at a separation of a, three (12) interactions at a separation of $a/\sqrt{3}$, three (12) interactions at a separation of $2a/\sqrt{3}$ and six (12) interactions at a separation of $\sqrt{\frac{7}{3}}a$. The three (12) interactions at a separation of $a/\sqrt{3}$ are due to the strong covalent bonds while the remaining interactions are due to the weak van der Waals forces. Figures 2(b) and 2(c) show the out-of-plane carbon-carbon interactions. There are two (13) interactions at a separation of $\frac{1}{2}c$ and six (14), six (23), and six (24) interactions at a separation of $(\frac{1}{4}c^2 + \frac{1}{3}a^2)^{1/2}$. The interactions given in Fig. 2 are considered to be significant and all have separations less than 4 Å.

In studying the dynamics of a crystalline lattice the dynamical matrix $\underline{M}$ is defined in terms of the force constants $\phi_{xy}(l', \overline{kk'})$ as

$$M_{xy}(\vec{q}, kk') = M_{xy}(\vec{q}, kk') - \delta'_{kk}\sum_{k''}\bar{M}_{xy}(0, kk'')\,, \tag{2}$$

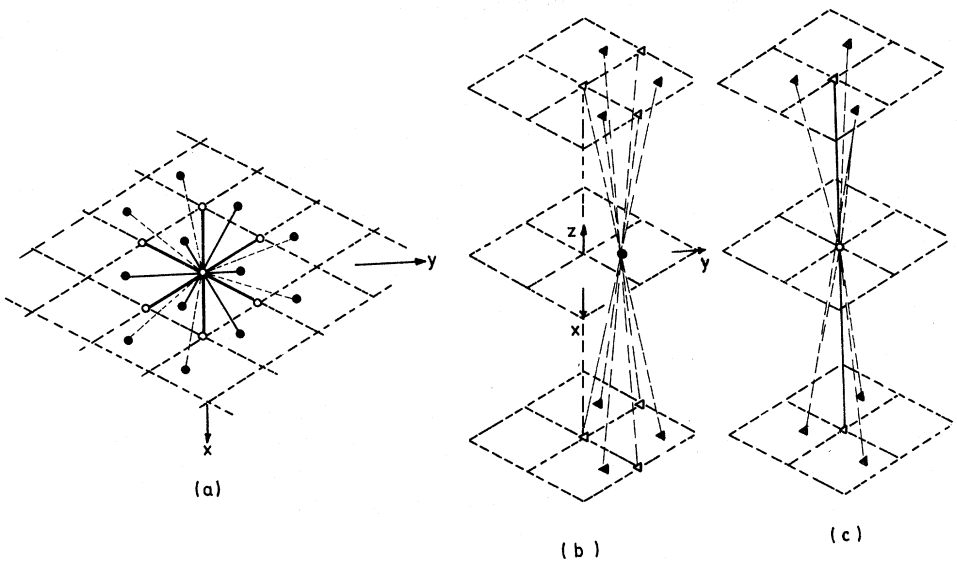

FIG. 2. Using the notation of Fig. 1, (a) the in-plane neighbors of carbon 1, (b) the out-of-plane neighbors of carbon 2, and (c) the out-of-plane neighbors of carbon 1. The neighbors of all carbon atoms can be constructed from the information given here and the graphite crystal symmetry.

where

$$\bar{M}_{xy}(\vec{q}, kk') = \sum_{l'}{}' \phi_{xy}(l', kk')\, e^{i\vec{q}\cdot\vec{r}^{\,l'}_{kk'}} . \tag{3}$$

The indices k and k' represent the atoms in a unit cell, $\vec{r}^{\,l'}_{kk'} = \vec{r}(l'k') - \vec{r}(0k)$, with $\vec{r}(lk)$ being the position of the atom k in the unit cell l. Defining $\vec{r} = \vec{r}^{\,l'}_{kk'}$, the force constants $\phi_{xy}(l', kk')$ are given by

$$\phi_{xy}(l', kk') = \left(-\delta_{xy} + \frac{r_x r_y}{r^2}\right)\frac{1}{r}\frac{dV}{dr} - \frac{r_x r_y}{r^2}\frac{d^2V}{dr^2} \tag{4}$$

if $V(r)$ is the potential of interaction between the two atoms k and k'. The interaction potential $V(r)$ will be assumed to have the Lennard–Jones form:

$$V(r) = 4\epsilon[(\sigma/r)^{12} - (\sigma/r)^6] \tag{5}$$

making the dynamical matrix $\underline{M}$ a function of the potential parameters σ and ϵ. The diagonalization of $\underline{M}$ at different wave vectors $\vec{q}$ using the equation of motion

$$\underline{m}\omega^2\vec{U} = \underline{M}\vec{U} \tag{6}$$

will provide the dispersion relations $\omega(\vec{q})$ and the polarization vectors $\vec{U}$.

In general the force constants $\phi_{xy}(l', kk')$ can be treated as adjustable parameters and fitted to the experimental data if the use of an interaction potential $V(r)$, as suggested above, is not considered. The force constants ϕ_{xy} are usually large in number and due to limited experimental data, it is desirable to reduce the number of these force constants as much as possible. One method of force-constant reduction is the use of the point-group symmetry of the crystal. The force-constant matrix $\underline{\phi}$, being a property of the crystal, transforms under a symmetry operation $\underline{S}$ belonging to the point group of crystal in the form

$$\underline{\phi}(l, kk') = \underline{S}\,\underline{\phi}(L, KK')\underline{S}^T . \tag{7}$$

It is obvious that if the indices $l\,kk'$ and $L\,KK'$ become identical, Eq. (7) provides relations among the force constants of kk' interaction, hence reducing the number of the unknown force constants. In other words, if an interaction is invariant under a symmetry operation $\underline{S}$, its force constants can be reduced in number using Eq. (7).

The graphite space group is given as C^4_{6v} by Wyckoff.[13] There are, however, recent studies of the graphite structure which suggest the possibility of the D^4_{6h} space-group symmetry.[14] We will not show preference for either one of the space groups and will try to generalize our calculations such that the effects of both space groups are included.

The space group C^4_{6v} contains the symmetry operations of identity E, two $C_3(z)$, and three σ_v, where one corresponds to the yz plane of Figs. 1 and 2 and the other two are placed 120° apart. In addition, there are three glide planes $[\sigma_v|\frac{1}{2}c]$ which include the z axis and are located 30° from σ_v planes. There are also one twofold screw axis $[C_2(z)|\frac{1}{2}c]$ and two sixfold screw axes $[C^{\pm1}_6(z)|\frac{1}{2}c]$. The space group D^4_{6h} contains 24 elements which are the result of the direct product of the 12 elements of C^4_{6v} space group with the group C_i which contains the identity and inversion symmetry operations. In what follows, we will consider the symmetry reductions of the typical force-constant matrix of an interaction using the symmetry operations of the space group C^4_{6v} since the addition of the center of inversion will not influence the symmetry reductions and the results will be valid for D^4_{6h} space group as well. One can obtain the expressions for all of the force-constant matrices using the given typical force-constant matrices

and Eq. (7).

The in-plane (11), (22), (33), and (44) interactions have the same positions and separations as given in Fig. 2(a) for the (11) interaction. The general form of their force constant matrix is

$$\underline{\phi}(100, kk) = \begin{pmatrix} \phi_{xx} & \phi_{xy} & \phi_{xz} \\ \phi_{yx} & \phi_{yy} & \phi_{yz} \\ \phi_{zx} & \phi_{zy} & \phi_{zz} \end{pmatrix}, \quad k = 1, 2, 3, 4 . \tag{8}$$

However, these nine force constants are not independent. For example, using the twofold screw axis and Eq. (7), $\underline{\phi}(100, 11)$ is related to $\underline{\phi}(\bar{1}00, 33)$ and by virtue of the sixfold screw axis and Eq. (7), $\underline{\phi}(010, 11)$ and $\underline{\phi}(1\bar{1}0, 33)$ are related. Using the full reduction by the screw axes and glide planes, it can be readily shown that

$$\underline{\phi}(100, kk) = \begin{pmatrix} \alpha_1 & \frac{1}{2}\sqrt{3}\,(\beta_1 - \alpha_1) & 0 \\ \frac{1}{2}\sqrt{3}\,(\beta_1 - \alpha_1) & \beta_1 & 0 \\ 0 & 0 & \gamma_1 \end{pmatrix}, \quad k = 1, 2, 3, 4 \tag{9}$$

where $\alpha_1 = \phi_{xx}(100, kk)$, $\beta_1 = \phi_{yy}(100, kk)$, and $\gamma_1 = \phi_{zz}(100, kk)$.

The three (12) interactions at $a/\sqrt{3}$ separation are invariant under σ_v symmetry operations resulting in

$$\underline{\phi}(\tfrac{1}{3}\,\tfrac{1}{3}0, 12) = \begin{pmatrix} \alpha_2 & 0 & 0 \\ 0 & \beta_2 & \nu_2 \\ 0 & \nu_2 & \gamma_2 \end{pmatrix}, \tag{10}$$

where $\alpha_2 = \phi_{xx}(\frac{1}{3}\,\frac{1}{3}0, 12)$, $\beta_2 = \phi_{yy}(\frac{1}{3}\,\frac{1}{3}0, 12)$, $\gamma_2 = \phi_{zz}(\frac{1}{3}\,\frac{1}{3}0, 12)$, and $\nu_2 = \phi_{yz}(\frac{1}{3}\,\frac{1}{3}0, 12)$. The three (12) interactions at $2a/\sqrt{3}$ separation show the same type of invariancy under σ_v symmetry operations and have a force-constant matrix of the form

$$\underline{\phi}(\bar{\tfrac{2}{3}}\,\bar{\tfrac{2}{3}}0, 12) = \begin{pmatrix} \alpha_3 & 0 & 0 \\ 0 & \beta_3 & \nu_3 \\ 0 & \nu_3 & \gamma_3 \end{pmatrix}, \tag{11}$$

where $\alpha_3 = \phi_{xx}(\bar{\frac{2}{3}}\,\bar{\frac{2}{3}}0, 12)$, $\beta_3 = \phi_{yy}(\bar{\frac{2}{3}}\,\bar{\frac{2}{3}}0, 12)$, $\gamma_3 = \phi_{zz}(\bar{\frac{2}{3}}\,\bar{\frac{2}{3}}0, 12)$, and $\nu_3 = \phi_{yz}(\bar{\frac{2}{3}}\,\bar{\frac{2}{3}}0, 12)$. The six (12) interactions at a separation of $\sqrt{\frac{7}{3}}\,a$ have no symmetry reduction and their force constants are of the form

$$\underline{\phi}(\tfrac{4}{3}\,\tfrac{1}{3}0, 12) = \begin{pmatrix} \alpha_4 & \eta_4 & \xi_4 \\ \eta_4 & \beta_4 & \nu_4 \\ \xi_4 & \nu_4 & \gamma_4 \end{pmatrix}, \tag{12}$$

where $\alpha_4 = \phi_{xx}(\frac{4}{3}\,\frac{1}{3}0, 12)$, $\beta_4 = \phi_{yy}(\frac{4}{3}\,\frac{1}{3}0, 12)$, $\gamma_4 = \phi_{zz}(\frac{4}{3}\,\frac{1}{3}0, 12)$, $\eta_4 = \phi_{xy}(\frac{4}{3}\,\frac{1}{3}0, 12)$, $\xi_4 = \phi_{xz}(\frac{4}{3}\,\frac{1}{3}0, 12)$, and $\nu_4 = \phi_{yz}(\frac{4}{3}\,\frac{1}{3}0, 12)$. The (34) force constants are readily obtained from the (12) force constants using the screw axis and glide-plane symmetry operations along with Eq. (7).

The (13) interaction is invariant under σ_v and $C_3(z)$ symmetry operations resulting in the force-constant matrix of the form

$$\underline{\phi}(00\tfrac{1}{2}, 13) = \begin{pmatrix} \alpha_5 & 0 & 0 \\ 0 & \alpha_5 & 0 \\ 0 & 0 & \gamma_5 \end{pmatrix}, \tag{13}$$

where $\alpha_5 = \phi_{xx}(00\frac{1}{2}, 13)$ and $\gamma_5 = \phi_{zz}(00\frac{1}{2}, 13)$. The (14), (24), and (23) interactions are all invariant under σ_v symmetry operations and have identical geometry and separations. The typical force constant has the form

$$\underline{\phi}(\bar{\tfrac{1}{3}}\,\tfrac{1}{3}\,\tfrac{1}{2}, 23) = \begin{pmatrix} \alpha_6 & 0 & 0 \\ 0 & \beta_6 & \nu_6 \\ 0 & \nu_6 & \gamma_6 \end{pmatrix}, \tag{14}$$

where $\alpha_6 = \phi_{xx}(\bar{\frac{1}{3}}\,\frac{1}{3}\,\frac{1}{2}, 23)$, $\beta_6 = \phi_{yy}(\bar{\frac{1}{3}}\,\frac{1}{3}\,\frac{1}{2}, 23)$, $\gamma_6 = \phi_{zz}(\bar{\frac{1}{3}}\,\bar{\frac{1}{3}}\,\frac{1}{2}, 23)$, and $\nu_6 = \phi_{yz}(\bar{\frac{1}{3}}\,\frac{1}{3}\,\frac{1}{2}, 23)$.

In using central two-body potentials of interaction some of the force constants will have a value of zero. These include ν_2, ν_3, ξ_4, and ν_4. In writing the dynamical matrix elements according to Eq. (2), we will set these force constants equal to zero and do not include them in the dynamical matrix. The dynamical matrix elements are summarized in Appendix A.

III. POTENTIALS OF INTERACTION

There are two types of carbon-carbon interactions in graphite. In each sheet the interactions of a carbon atom with its three nearest-neighbor carbon atoms are through strong covalent forces. These correspond to the force constants α_2, β_2, and γ_2. The rest of the interactions, including the out-of-sheet interactions, are all due to the van der Waals forces. Hence only two types of potentials are needed in order to fully specify the carbon-carbon interactions in graphite.

For the carbon-carbon van der Waals potential we made use of the similarities of carbon and nitrogen atoms. The electronic structure of carbon atom ($M = 12$, $Z = 6$, $1s^2\,2s^2\,2p^2$) and nitrogen atom ($M = 14$, $Z = 7$, $1s^2\,2s^2\,2p^3$) are very similar and it is believed that the carbon-carbon and nitrogen-nitrogen van der Waals potentials of interaction will be very much the same. The potential parameters for the nitrogen-nitrogen van der Waals interactions are obtained by Kuan, Warshel, and Schnepp[15] from various intermolecular potentials of solid α-N_2. From conditions of zero uniform stress and

TABLE I. Character table and selection rules for crystalline graphite. Raman (R) and infrared (ir) activity are specified by a for allowed transitions and f for forbidden transition.

c_{6v}	E	c_2	$2c_3$	$2c_6$	$3\sigma_v$	$3\sigma_d$	n_i	n_i'	n_T	R	ir
A_1	1	1	1	1	1	1	3	2	1	a	a
A_2	1	1	1	1	−1	−1	0	0	0	f	f
B_1	1	−1	1	−1	1	−1	1	1	0	f	f
B_2	1	−1	1	−1	−1	1	0	0	0	f	f
E_1	2	−2	−1	1	0	0	3	2	1	a	a
E_2	2	2	−1	−1	0	0	1	1	0	a	f
U_R	4	2	2	2	4	2					
ϕ	0°	180°	120°	60°	0	0					
$\pm 1+2\cos\phi$	3	−1	0	2	1	1					
$U_R(\pm 1+2\cos\phi)$	12	−2	0	4	4	2					
$2\cos\phi(\pm 1+2\cos\phi)$	6	2	0	2	2	2					

the experimental lattice energy they obtain

$$\sigma = 3.345 \text{ Å}, \quad \epsilon = 37 \text{ °K}. \tag{15}$$

We will assume these values to be the same as the carbon-carbon van der Waals potential parameters.

The covalent force constants or the parameters of a potential for covalent forces can be obtained from the long-wavelength frequencies of graphite. The information on the complete set of the long-wavelength frequencies of graphite is lacking at present and only two of the normal mode frequencies have been observed and assigned.[8,16] In our calculations we will consider an alternative route in estimating the long-wavelength frequencies of graphite and will compare our results with the available measurements. The long-wavelength frequencies will then be used to calculate the potential parameters of the covalent forces.

The atoms within a sheet of graphite have a structure much like the atoms in a benzene molecule. The benzene molecule is a well studied molecule with many of its normal-mode frequencies established in frequency and assignment.[17] Since a benzene ring has the same structure of carbon atoms as the carbon atoms in a sheet of graphite, it is possible to do a group-theoretical analysis of graphite and compare it with the group-theoretical analysis of the benzene molecule. From this comparison approximate values for the long-wavelength frequencies of graphite can be obtained using the measurements available on the benzene molecule.

The character table and the selection rules for graphite crystal, with the point group C_{6v}, are given in Table I. The number of the normal modes of various types and their activity in the infrared and Raman spectra are obtained from the relevant equations[18,19] and the character tables. n_i is the total number of normal modes under a symmetry species i, n_i' is the number of internal vibration modes with n_T being the number of pure translations under a symmetry species. Raman and infrared activity of a mode are specified by letters a and f designating allowed and forbidden transitions, respectively.

It is seen from Table I that there are two active modes of species A_1 and two active modes of species E_1. From a study of the dynamical matrix at $\vec{q}=0$ and the relative magnitudes of the covalent and van der Waals force constants it can be shown that for all practical purposes the frequencies of the two species A_1 are degenerate in value and so are the frequencies of the two species E_1. Hence, in comparing our group-theoretical results with those of the benzene molecule, those frequencies that first involve the relative movement of carbon atoms, and second satisfy the above degeneracy requirement, must be chosen for the graphite-normal-mode frequencies of vibration.

The group-theoretical analysis of benzene molecule assuming C_{6v} point-group symmetry is available[17] and the comparison of its symmetry species with those of graphite are given in Table II. It is interesting to note that the frequencies given in Table II not only satisfy the symmetry requirements, but they show the expected degeneracy of graphite frequencies of A_1 and E_1 species. The values chosen for graphite-normal-mode frequencies are taken as the averages of the frequencies of benzene molecule. These are

$$\omega(A_1) = 1000 \text{ cm}^{-1}, \quad \omega(E_1) = 1550 \text{ cm}^{-1}. \tag{16}$$

The above values are supported by the recent measurements of Brillson *et al.*[18] of

$$\omega(E_1) = 1588 \pm 5 \text{ cm}^{-1} \text{ and } \omega(E_2) = 1574 \pm 1 \text{ cm}^{-1}. \tag{17}$$

The frequencies in Eqs. (16) provide us with sufficient information about the potential parameters of the carbon-carbon covalent interactions. Expressing the force constants α_2 and β_2 in terms of a two-body interaction potential, we obtained

$$\sigma = 1.174 \text{ Å}, \quad \epsilon = 6.35\times10^4 \text{ °K}. \tag{18}$$

It should be pointed out that the group-theoretical treatment of graphite using D_{6h}^4 space-group symmetry[18] and of the benzene molecule using D_{6h} point-group symmetry[17] result in the same conclusions as given in Eqs. (16). These calculations will

TABLE II. Comparison of graphite and benzene-molecule symmetry species assuming c_{6v} point group.

Benzene molecule	Graphite	Benzene-molecule frequency (cm^{-1})[a]
A_1	A_1	991.6
B_1	A_1	1008
E_1	E_1	1485
E_2	E_1	1584.8

[a]Reference 16.

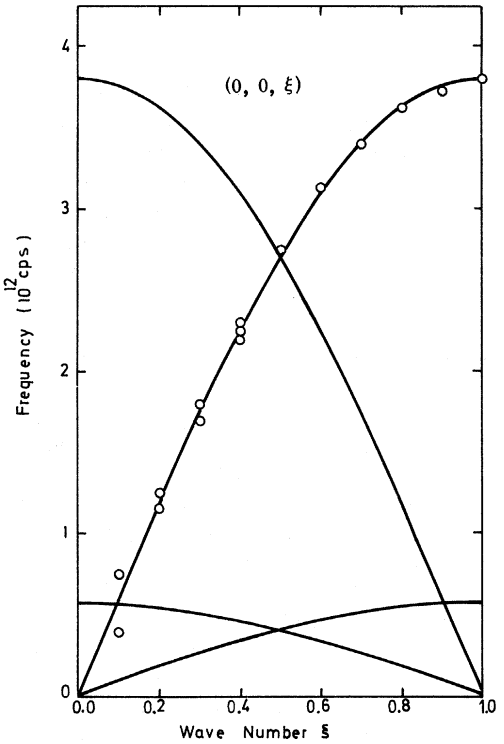

FIG. 3. Comparison of the calculated (solid line) dispersion curves and the experimental observations (full circles) along (0, 0, ξ).

not be repeated here and in the following sections we will calculate various properties of graphite, using potentials of Eqs. (15) and (18), and compare the results with the available experimental data.

IV. DISPERSION CURVES AND STRUCTURE FACTORS

Using the carbon-carbon interaction potentials the dispersion relations along (0, 0, ξ), (0, ξ, 0), and (ξ, 0, 0) are calculated. Dolling and Brockhouse[8] have measured the dispersion curve along (0, 0, ξ) which is assumed to be the longitudinal acoustic branch. Our theoretical calculations are compared with these experimental data in Fig. 3 showing an excellent agreement between the two. This agreement gives support to the assumptions made in Sec. III in connection with the carbon-carbon potentials of interaction. It is observed from the polarization vectors along (0, 0, ξ) that the dispersion curve in Fig. 3 is the longitudinal acoustic branch up to (0, 0, $\frac{1}{2}$) and the longitudinal optic branch from (0, 0, $\frac{1}{2}$) to (0, 0, 1). The two high-frequency modes, not shown in Fig. 3, have values of $\omega(E_1) = 46.6 \times 10^{12}$ Hz and $\omega(A_1) = 30.1 \times 10^{12}$ Hz corresponding to 1550 and 1000 cm^{-1}, respectively, and are δ functions along (0, 0, ξ) with no dispersion.

The dispersion curves along (ξ, 0, 0) and (0, ξ, 0) directions are given in Fig. 4. The frequencies of the acoustic branches reach considerably higher values compared to the acoustic branches along (0, 0, ξ) direction. This is explained by the difference in the nature of interaction forces along and perpendicular to the z axis of graphite. Because of the large scale of frequencies in Fig. 4, the $\vec{\xi} = 0$ transverse-optic frequency at 0.567×10^{12} Hz is seen very similar to an acoustic mode.

The dispersion relation $\omega(\vec{q})$ is measured by inelastic coherent scattering of neutrons from single-crystal specimens. The condition of finite-scattering cross section is satisfied if the structure factor[20]

$$S_F = \left(\sum_k \frac{\bar{b}_k}{M_k^{1/2}} e^{i\vec{Q}\cdot\vec{R}_k} \vec{Q}\cdot\vec{U}(k) e^{-W_k} \right)^2 \qquad (19)$$

has a nonzero value. $\bar{b}_k$ is the coherent scattering amplitude, M_k is the atomic mass, $\vec{R}_k$ is the position, $\vec{U}(k)$ is the atomic displacement from equilibrium, and W_k is the Debye–Waller factor asso-

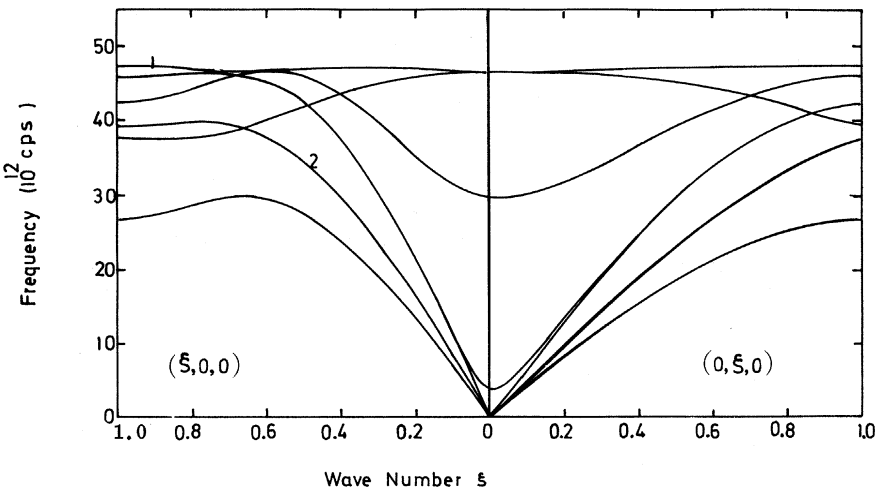

FIG. 4. Calculated dispersion curves of graphite along (0, ξ, 0) and (ξ, 0, 0).

ciated with the kth atom in the unit cell.

Considering that only carbon atoms are present in graphite and assuming that the Debye–Waller factor is close to unity, we define the structure factor in the form

$$S_F = \frac{1}{Q^2}\left(\sum_k e^{i\vec{Q}\cdot\vec{R}_k}\vec{Q}\cdot\vec{U}(k)\right)^2 , \tag{20}$$

where

$$\vec{Q} = 2\pi\vec{\tau} \pm \vec{q} . \tag{21}$$

$\vec{\tau}$ is the reciprocal-lattice vector of graphite given by

$$\vec{\tau} = h\vec{b}_1 + k\vec{b}_2 + l\vec{b}_3 , \tag{22}$$

where hkl are integers and b_i are the reciprocal lattice vectors

$$\vec{b}_1 = \frac{1}{a}\hat{x} + \frac{1}{\sqrt{3}a}\hat{y} ,$$
$$\vec{b}_2 = -\frac{1}{a}\hat{x} + \frac{1}{\sqrt{3}a}\hat{y} , \tag{23}$$
$$\vec{b}_3 = \frac{1}{c}\hat{z} .$$

The phonon wave vector $\vec{q}$ is defined as

$$\vec{q} = 2\pi\left(\frac{1}{a}\xi_x\hat{x} + \frac{1}{\sqrt{3}a}\xi_y\hat{y} + \frac{1}{c}\xi_z\hat{z}\right) , \tag{24}$$

where the components of $\vec{\xi}$ vary between zero and one.

The calculated structure factors along $(\xi, 0, 0)$ and $(0, 0, \xi)$ directions are plotted in Fig. 5 as a function of $\vec{Q}$. It is interesting to note that the structure factor along $(\xi, 0, 0)$ is independent of the choice of Q_x and it depends only on the phonon wave vector q_x. The same branches are marked with the same integers on the dispersion curves and the structure-factor curves. The structure factor along $(0, 0, \xi)$ has a value of zero for the longitudinal-optic mode $\xi = 1.0$ meaning that the optical phonon at (0, 0, 1) should not be observed. The (0, 0, 1) phonon observed by Dolling and Brockhouse, on the contrary, is quite sharp. This discrepancy in part may be due to the imperfect graphite crystals used in the experiment.

V. ELASTIC CONSTANTS

The elastic constants of graphite are calculated using the method of long waves.[21] We will not go into details of these calculations and only give the

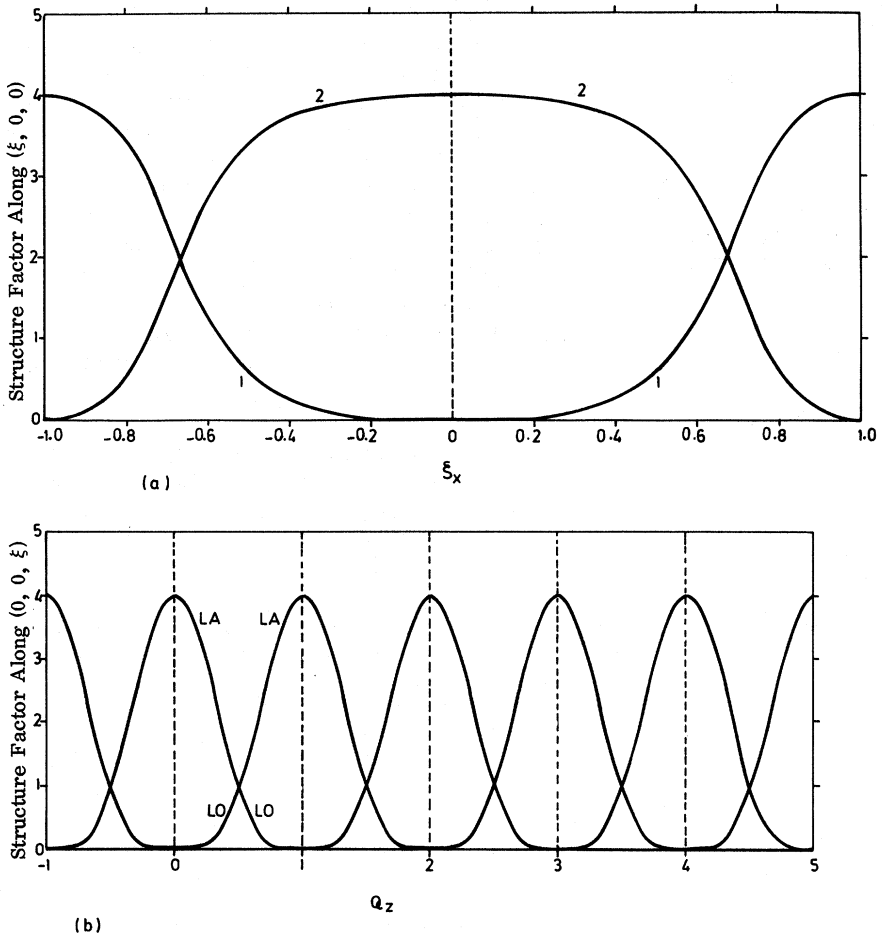

FIG. 5. Calculated structure factors of graphite along $(\xi, 0, 0)$ and $(0, 0, \xi)$. The number on a structure-factor curve refers to a corresponding dispersion curve in Fig. 4.

results for a solid in which the interactions between atoms are through central forces. The elastic constants $c_{\alpha\gamma\beta\lambda}$ are defined as

$$c_{\alpha\gamma\beta\lambda}=f_{\alpha\beta\gamma\lambda}+g_{\alpha\gamma\beta\lambda}\ . \tag{25}$$

Denoting the atomic separations $\vec{r}^{\,l'}_{kk'}$ by $\vec{r}$ and the derivatives of the interaction potentials $dV(r)/dr^2$ and $d^2V(r)/d(r^2)^2$ by V' and V'', respectively, the functions $f_{\alpha\beta\gamma\lambda}$ and $g_{\alpha\gamma\beta\lambda}$ are given by

$$f_{\alpha\beta\gamma\lambda}=\frac{2}{v_a}\sum_{l'kk'}{}' r_\alpha r_\beta r_\gamma r_\lambda V'' \tag{26}$$

and

$$g_{\alpha\gamma\beta\lambda}=\frac{-1}{v_a}\sum_{kk'}\sum_{\mu\nu}P_{\mu\nu}(kk')\left(\sum_{k''}M_{\mu\alpha\gamma}(kk'')\right)\times\left(\sum_{k'''}M_{\nu\beta\lambda}(k'k''')\right),$$

where

$$M_{\alpha\beta\gamma}(kk')=\frac{2}{(m_k)^{1/2}}\left(\delta_{\alpha\beta}\sum_{l'}r_\gamma V'+2\sum_{l'}r_\alpha r_\beta r_\gamma V''\right). \tag{27}$$

v_a is the unit cell volume and the matrix $P_{\mu\nu}(kk')$ is the inverse of the matrix $N_{\alpha\beta}(kk')$ where

$$N_{\alpha\beta}(kk')=\frac{1}{(m_k m_{k'})^{1/2}}\left(-2\delta_{\alpha\beta}\sum_{l'}V'-4\sum_{l'}r_\alpha r_\beta V''\right) \qquad k\neq k'$$

$$=\frac{1}{m_k}\left(2\delta_{\alpha\beta}\sum_{l'k'}{}'V'+4\sum_{l'k'}{}'r_\alpha r_\beta V''\right), \quad k=k'\ . \tag{28}$$

It can be very easily shown that for the elastic constants c_{11}, c_{12}, c_{13}, c_{44}, c_{33}, and c_{66} the $f_{\alpha\beta\gamma\lambda}$ are all finite valued and satisfy the Cauchy relations, i.e.,

$$f_{13}=f_{44}\ ,\quad f_{12}=f_{66}\ . \tag{29}$$

The calculations of $g_{\alpha\gamma\beta\lambda}$ show that it is nonzero only for c_{11} and c_{12} elastic constants and that

$$g_{11}=g_{12}\ . \tag{30}$$

$g_{\alpha\gamma\beta\lambda}$ for c_{13}, c_{33}, c_{44}, and c_{66} is identically zero. The value of g_{11} is given by

$$g_{11}=(-1/v_a)\,[P_{yy}(33)+P_{yy}(44)-2P_{yy}(34)]\times[M_{yxx}(14)+M_{yxx}(12)]^2 \tag{31}$$

where

$$P_{yy}(33)=\frac{1}{|\vec{\mathrm{N}}|}\begin{vmatrix}N_{yy}(22) & N_{yy}(23)\\ N_{yy}(23) & N_{yy}(44)\end{vmatrix}\ ,$$

$$P_{yy}(44)=\frac{1}{|\vec{\mathrm{N}}|}\begin{vmatrix}N_{yy}(22) & N_{yy}(23)\\ N_{yy}(23) & N_{yy}(33)\end{vmatrix}\ , \tag{32}$$

$$P_{yy}(34)=\frac{-1}{|\vec{\mathrm{N}}|}\begin{vmatrix}N_{yy}(22) & N_{yy}(23)\\ N_{yy}(23) & N_{yy}(34)\end{vmatrix}\ ,$$

with

$$|\vec{\mathrm{N}}|=\begin{vmatrix}N_{yy}(22) & N_{yy}(23) & N_{yy}(23)\\ N_{yy}(23) & N_{yy}(33) & N_{yy}(34)\\ N_{yy}(23) & N_{yy}(34) & N_{yy}(44)\end{vmatrix}\ . \tag{33}$$

Table III provides the comparison between the calculated and experimental[12] elastic constants revealing good agreement in c_{33} and c_{44} and showing poor agreement in c_{11}, c_{12}, c_{13}, and c_{66}. It is interesting to note that the theoretical results satisfy the Cauchy relation $c_{13}=c_{44}$ which is not observed experimentally. In the experimental observations c_{11} and c_{12} have a ratio of 6:1 while Eq. (25) gives a 3:1 ratio essentially independent of the magnitude of the interaction forces.

In an attempt to explain the observed discrepancies we calculated the Young moduli of graphite for the two sets of values in Table III assuming a polycrystalline graphite with random distribution of the grain orientations. Using the *VRH* approximation[22,23] which relates the single-crystal data to the values of polycrystalline data, we obtained a value of 40×10^{11} dyn/cm^2 for our calculations and a value of 17×10^{11} dyn/cm^2 for the experimental values in Table III. This compares with the observed average Young modulus of graphite of $\sim1\times10^{11}$ dyn/cm^2.[7] It should be pointed out that the *VRH* approximation has been quite satisfactorily applied to a large number of materials of cubic, tetragonal, and trigonal symmetries[23,24] so long as the density of the polycrystalline specimen is sufficiently close to the theoretical value. In the case of graphite, Young moduli have been experimentally measured using specimens with densities considerably different from the theoretical value of 2.26 g/cm^3. Although this may explain the difference between the values of Young moduli, the reason for discrepancies in our calculated elastic constants and the experimental observations is not clearly known.

VI. DISCUSSION

The lattice vibrations of the hexagonal graphite crystal are studied using two-body analytical potentials of interaction of the Lennard–Jones type. The potential parameters of the covalent interactions are

TABLE III. Observed elastic constants (in 10^{11} dyn/cm^2) of graphite and the corresponding values calculated from Eq. (25).

Elastic constant	Observed	$f_{\alpha\beta\gamma\lambda}$	$g_{\alpha\gamma\beta\lambda}$	$c_{\alpha\gamma\beta\lambda}$
c_{11}	106 ± 2	230.4	−3.15	227.2
c_{12}	18 ± 2	76.8	−3.15	73.6
c_{66}	44 ± 2	76.8	0	76.8
c_{33}	3.65 ± 0.1	3.8	0	3.8
c_{13}	1.5 ± 0.5	0.22	0	0.22
c_{44}	≥0.4	0.22	0	0.22

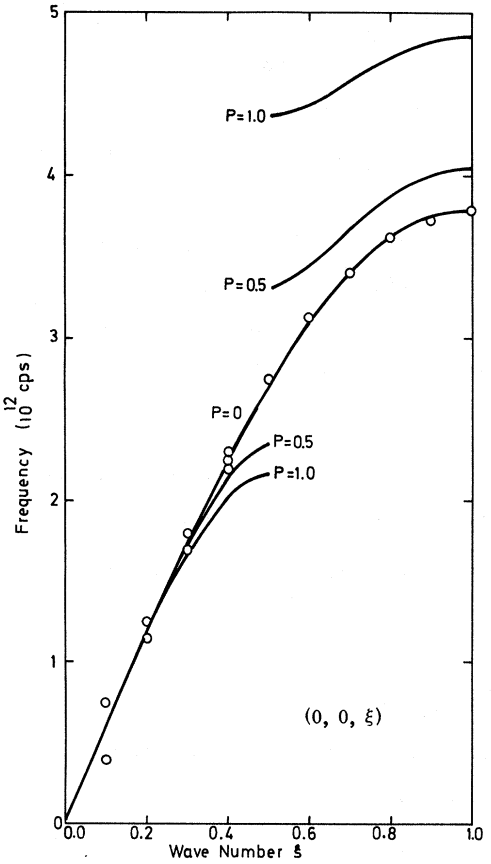

FIG. 6. Structure dependence of the dispersion curves of graphite crystal along (0, 0, ξ).

obtained from the long-wavelength frequencies of graphite. These are in turn estimated from the internal frequencies of benzene molecule. The carbon-carbon van der Waals potential is obtained from the two-body interaction potential of nitrogen atoms which are very similar to the carbon atoms in size and the electronic structure. Using the two-body carbon-carbon potentials, a number of properties of the graphite are calculated. These include the dispersion relations and the elastic constants. In calculating any property, the comparison generally shows excellent agreement whenever experimental observations are available. The good agreement is not unexpected since similar models[9–11] using two-body potentials of interaction have been quite successful.

Although the assumed model has shown itself to be quite reliable, we considered the possibility of a deviation from the assumed graphite structure which is mentioned by Wyckoff.[13] He states that the position of the carbon atoms 2 and 4 may not be in the same plane as the atoms 1 and 3 and gives the position vectors of 000, $\frac{1}{3}\frac{1}{3}v$, $00\frac{1}{2}$, $\frac{2}{3}\frac{2}{3}\frac{1}{2}+v$ for atoms 1 through 4, respectively. The value of v is stated to be zero for practical purposes, and cannot exceed 5% of c in value.

It was hence decided to set up a model in which the carbon atoms 2 and 4 have a displacement v varying from zero up to a value of $0.05c$. This means a reconstruction of the force constants and a new dynamical matrix since the changing distances produce not only asymmetry in interactions but also introduce a larger number of force constants. The increase in the number of force constants will not be troublesome since they are readily determined using the two-body interaction potentials. The new dynamical matrix is set up and diagonalized along (0, 0, ξ) for three values of $P = v/0.05 = 0, \frac{1}{2}$, and 1. The results given in Fig. 6 show the sensitivity of the dispersion curves to small structural changes and also indicate that for all practical purposes v is zero and the positions of the carbon atoms are in a single plane.

It should be pointed out that our treatment of graphite is essentially a rigid atom one. A better model of graphite will be through a shell-model[25] consideration of the carbon atoms. The shell model of graphite is supported by the observation of infrared-active modes.[16] Although carbon atoms do not have a static charge, the infrared activity of graphite modes is indicative of the deformation of the charge distribution[26] of the carbon atoms which can only be accounted for by a shell-model lattice-dynamical treatment. Since a good fitting of the experimental data with the shell model requires the use of a rather large number of unknown adjustable parameters, we believe that a shell-model treatment of graphite will be possible only when detail dispersion data exist through neutron-scattering experiments.

In conclusion we would like to emphasize the usefulness of the two-body potentials in the analysis of lattice vibrations of crystalline solids. A knowledge of the interaction potentials can be obtained from a variety of measurements.[27] The potential approach is most useful in studying crystalline solids where the available information is limited, or in studies where the large number of atoms per unit cell complicates the picture even though there is a reasonable amount of data available. It is also of interest to note that by using the two-body analytical potentials one can avoid the problem of fitting the force constants to the available data which is shown to be possible for a wide range of alternative sets of force constants.[28]

ACKNOWLEDGMENTS

We would like to thank Dr. M. Mohajeri for programming assistance and Pahlavi University Computation Center for computer time. One of us (HAR) is indebted to Dr. M. Shahinpoor for one very useful suggestion.

APPENDIX A

The dynamical matrix elements $M_{xy}(\vec{q}, kk')$ of graphite are listed here. For the sake of simplicity the wave vector $\vec{q}$ in the argument of the dynamical matrix elements is suppressed.

$$M_{xx}(11) = 4\alpha_1(c_1c_2 - 1) + (6\beta_1 - 2\alpha_1)(c_1^2 - 1) - D_1$$
$$\equiv f(\alpha_1, \beta_1, D_1),$$
$$M_{yy}(11) = f(\beta_1, \alpha_1, D_1),$$
$$M_{zz}(11) = 4\gamma_1(c_1^2 + c_1c_2 - 2) - D_2 \equiv g(\gamma_1, D_1),$$
$$M_{xy}(11) = \sqrt{3}(\alpha_1 - \beta_1)S_1S_2, \quad M_{xz}(11) = M_{yz}(11) = 0,$$
$$M_{ij}(33) = M_{ij}(11), \qquad i, j = x, y, z$$
$$M_{xx}(22) = f(\alpha_1, \beta_1, D_3), \quad M_{yy}(22) = f(\beta_1, \alpha_1, D_3),$$
$$M_{zz}(22) = f(\gamma_1, D_4),$$
$$M_{xy}(22) = M_{xy}(11), \qquad M_{xz}(22) = M_{yz}(22) = 0,$$
$$M_{ij}(44) = M_{ij}(22), \qquad i, j = x, y, z$$
$$D_1 = 2\alpha_5 + 3(\alpha_4 + \beta_4) + \tfrac{3}{2}(\alpha_2 + \beta_2 + \alpha_3 + \beta_3 + 2\alpha_6 + 2\beta_6),$$
$$D_2 = 2\gamma_5 + 6\gamma_4 + 3(\gamma_2 + \gamma_3 + 2\gamma_6),$$
$$D_3 = 3(\alpha_4 + \beta_4) + \tfrac{3}{2}(\alpha_2 + \beta_2 + \alpha_3 + \beta_3) + 6(\alpha_6 + \beta_6),$$
$$D_4 = 6\gamma_4 + 3(\gamma_2 + \gamma_3) + 12\gamma_6,$$

$$M_{xx}(12) = \alpha_2c_4 + (\tfrac{1}{2}\alpha_2 + \tfrac{3}{4}\beta_2)(c_5 + c_6) + \alpha_3c_7 + (\tfrac{1}{2}\alpha_3 + \tfrac{3}{4}\beta_3)(c_8 + c_9) + \alpha_4(c_{10} + c_{11}) + (\tfrac{1}{4}\alpha_4 + \tfrac{3}{4}\beta_4)(c_{12} + c_{13} + c_{14} + c_{15})$$
$$+ \tfrac{1}{2}\sqrt{3}\eta_4(c_{12} - c_{13} + c_{14} - c_{15}) + i[\alpha_2S_4 + (\tfrac{1}{4}\alpha_2 + \tfrac{3}{4}\beta_2)(S_5 + S_6) + \alpha_3S_7 + (\tfrac{1}{4}\alpha_3 + \tfrac{3}{4}\beta_3)(S_8 + S_9)$$
$$+ \alpha_4(S_{10} + S_{11}) + (\tfrac{1}{4}\alpha_4 + \tfrac{3}{4}\beta_4)(S_{12} + S_{13} + S_{14} + S_{15}) + \tfrac{1}{2}\sqrt{3}\eta_4(S_{12} - S_{13} + S_{14} - S_{15})]$$
$$\equiv f(\alpha_2, \beta_2, \alpha_3, \beta_3, \alpha_4, \beta_4, \eta_4),$$
$$M_{yy}(12) = f(\beta_2, \alpha_2, \beta_3, \alpha_3, \beta_4, \alpha_4, -\eta_4),$$
$$M_{zz}(12) = \gamma_2(c_4 + c_5 + c_6) + \gamma_3(c_7 + c_8 + c_9) + \gamma_4(c_{10} + c_{11} + c_{12} + c_{13} + c_{14} + c_{15})$$
$$+ i[\gamma_2(S_4 + S_5 + S_6) + \gamma_3(S_7 + S_8 + S_9) + \gamma_4(S_{10} + S_{11} + S_{12} + S_{13} + S_{14} + S_{15})],$$
$$M_{xy}(12) = -\tfrac{1}{4}\sqrt{3}(\alpha_2 - \beta_2)(c_5 - c_6) - \tfrac{1}{4}\sqrt{3}(\alpha_3 - \beta_3)(c_8 - c_9) - \tfrac{1}{4}\sqrt{3}(\alpha_4 - \beta_4)(c_{12} + c_{13} - c_{14} - c_{15})$$
$$- 0.5\eta_4(-2c_{10} + 2c_{11} + c_{12} - c_{13} - c_{14} + c_{15}) + i[-\tfrac{1}{4}\sqrt{3}(\alpha_2 - \beta_2)(S_5 - S_6) - \tfrac{1}{4}\sqrt{3}(\alpha_3 - \beta_3)(S_8 - S_9)$$
$$- \tfrac{1}{4}\sqrt{3}(\alpha_4 - \beta_4)(S_{12} + S_{13} - S_{14} - S_{15}) - 0.5\eta_4(-2S_{10} + 2S_{11} + S_{12} - S_{13} - S_{14} + S_{15})],$$

$$M_{xz}(12) = M_{yz}(12) = 0,$$
$$M_{xy}(34) = M_{xy}^*(12) \text{ for all } x \text{ and } y,$$
$$M_{xx}(13) = 2\alpha_5c_3,$$
$$M_{yy}(13) = M_{xx}(13),$$
$$M_{zz}(13) = 2\gamma_5c_3,$$
$$M_{xx}(14) = 2c_3[\alpha_6c_4 + (\tfrac{1}{4}\alpha_6 + \tfrac{3}{4}\beta_6)(c_5 + c_6)]$$
$$- i2c_3[\alpha_6S_4 + (\tfrac{1}{4}\alpha_6 + \tfrac{3}{4}\beta_6)(S_5 + S_6)]$$
$$\equiv f(\alpha_6, \beta_6),$$
$$M_{yy}(14) = f(\beta_6, \alpha_6),$$
$$M_{zz}(14) = 2\gamma_6c_3(c_4 + c_5 + c_6) - i2\gamma_6c_3(S_4 + S_5 + S_6),$$
$$M_{xy}(14) = -\tfrac{1}{2}\sqrt{3}(\alpha_6 - \beta_6)(S_5 - S_6)(S_3 - ic_3),$$
$$M_{xz}(14) = -\sqrt{3}\,\nu_6(S_5 - S_6)(S_3 - ic_3),$$
$$M_{yz}(14) = \nu_6(2S_4 - S_5 - S_6)(S_3 - ic_3),$$
$$M_{xy}(23) = M_{xy}(14) \text{ for all } x \text{ and } y,$$
$$M_{xy}(24) = M_{xy}^*(23) \text{ for all } x \text{ and } y.$$

The c_i symbols are

$$c_1 = \cos\pi\xi_x, \qquad c_2 = \cos\pi\xi_y, \quad c_3 = \cos\pi\xi_z,$$
$$c_4 = \cos(\tfrac{2}{3}\pi\xi_y), \qquad c_5 = \cos(-\pi\xi_x - \tfrac{1}{3}\pi\xi_y),$$
$$c_6 = \cos(\pi\xi_x - \tfrac{1}{3}\pi\xi_y), \qquad c_7 = \cos(-\tfrac{4}{3}\pi\xi_y),$$
$$c_8 = \cos(2\pi\xi_x + \tfrac{2}{3}\pi\xi_y), \qquad c_9 = \cos(-2\pi\xi_x + \tfrac{2}{3}\pi\xi_y),$$
$$c_{10} = \cos(\pi\xi_x + \tfrac{5}{3}\pi\xi_y), \qquad c_{11} = \cos(-\pi\xi_x + \tfrac{5}{3}\pi\xi_y),$$
$$c_{12} = \cos(-3\pi\xi_x - \tfrac{1}{3}\pi\xi_y), \quad c_{13} = \cos(-2\pi\xi_x - \tfrac{4}{3}\pi\xi_y),$$
$$c_{14} = \cos(3\pi\xi_x - \tfrac{1}{3}\pi\xi_y), \qquad c_{15} = \cos(2\pi\xi_x - \tfrac{4}{3}\pi\xi_y).$$

The symbols S_i correspond to the sines of the same argument as the above given cosine functions.

[1]K. Komatsu and T. Nagamiya, J. Phys. Soc. Japan 6, 438 (1951).
[2]G. F. Newell, J. Chem. Phys. 23, 2431 (1955).
[3]G. R. Baldock, Phil. Mag. 1, 789 (1956).
[4]A. Yoshimori and Y. Kitano, J. Phys. Soc. Japan 11, 352 (1956).
[5]J. A. Young and J. U. Koppel, J. Chem. Phys. 42, 357 (1965).

[6]R. Nicklow, N. Walkabayashi, and H. G. Smith, Phys. Rev. 5, 4951 (1972).
[7]C. L. Mantell, *Carbon and Graphite Handbook* (Interscience, New York, 1968), p. 358.
[8]G. Dolling and B. N. Brockhouse, Phys. Rev. 128, 1120 (1962).
[9]G. S. Pawley, Phys. Status Solidi 20, 347 (1967).
[10]G. S. Pawley and S. J. Cyvin, J. Chem. Phys. 52, 4073 (1970).
[11]H. A. Rafizadeh, S. Yip, and H. Prask, J. Chem. Phys. 56, 5377 (1972).
[12]O. L. Blackslee *et al.*, J. Appl. Phys. 41, 3373 (1970).
[13]R. W. G. Wyckoff, *Crystal Structures*, 2nd ed. (Interscience, New York, 1968), Vol. 1, p. 26.
[14]W. Ruland, in *Chemistry and Physics of Carbon*, edited by P. L. Walker, Jr. (Marcel Dekker, New York, 1968), Vol. 4, p. 1.
[15]T. S. Kuan, A. Warshel, and O. Schnepp, J. Chem. Phys. 52, 3012 (1970).
[16]L. J. Brillson, E. Burnstein, A. A. Maradudin, and T. Stark, in *Physics of Semimetals and Narrow Gap Semiconductors*, edited by Carter and Bate (Pergamon, New York, 1971), p. 187.
[17]G. Herzberg, *Molecular Spectra and Molecular Structure*, II. *Infrared and Raman Spectroscopy*, 13th ed. (Van Nostrand, New York, 1968).
[18]E. V. Wilson, J. C. Decius, and P. C. Cross, *Molecular Vibrations* (McGraw-Hill, New York, 1955).
[19]S. Bhagavantam and T. Venkatarayudu, *Theory of Groups and its Application to Physical Problems* (Waltair, Andhra University, Hyderabad, India, 1951).
[20]G. Dolling and A. D. E. Woods, in *Thermal Neutron Scattering*, edited by P. A. Egelstaff (Academic, New York, 1965).
[21]M. Born and K. Huang, *Dynamical Theory of the Crystal Lattices* (Clarendon, Oxford, England, 1954).
[22]R. W. Hill, Proc. Phys. Soc. (London) A65, 349 (1952).
[23]O. L. Anderson, in *Physical Acoustics*, edited by W. P. Manson (Academic, New York, 1965), Vol. III B.
[24]D. H. Chung and W. R. Buessem, J. Appl. Phys. 38, 2535 (1967).
[25]W. Cochran, Proc. Roy. Soc. (London) A253, 260 (1959).
[26]R. Zallen, Phys. Rev. 173, 824 (1968).
[27]J. O. Hirshfelder, C. F. Curtiss, and R. B. Bird, *Molecular Theory of Gases and Liquids* (Wiley, New York, 1954).
[28]R. S. Leigh, B. Szigeti, and V. K. Tewary, Proc. Roy. Soc. A320, 505 (1971).

PHYSICAL REVIEW B VOLUME 7, NUMBER 10 15 MAY 1973

Ground State of the Exciton-Phonon System

Herbert B. Shore*
Department of Physics, University of California, San Diego, La Jolla, California 92037

Leonard M. Sander
Department of Physics, University of Michigan, Ann Arbor, Michigan 48104

(Received 25 October 1972)

The ground state of a model exciton-phonon Hamiltonian is studied using variational techniques. A single-exciton band is considered in the tight-binding model; the exciton is coupled to Einstein phonons through a short-range linear interaction. We first verify that a variational wave function corresponding to simple displacements of the lattice coordinates (analogous to the Lee–Low–Pines wave function for the polaron) leads to an unphysical result: For strong exciton-phonon coupling the effective mass of the excitons depends discontinuously on the parameters of the Hamiltonian. We obtain an improved trial function by studying an exactly soluble problem: an exciton hopping between two sites and coupled to a phonon field. The new trial function allows distortion of the Gaussian form of the phonon wave function as well as displacement. Analogous trial functions are used to calculate the energy and effective mass for a one-dimensional lattice with nearest-neighbor exciton hopping. The results are a continuous effective mass and a substantial improvement of the ground-state energy over the Lee–Low–Pines trial function. Arguments are given that the qualitative behavior of the ground state is independent of the dimensionality of the lattice, so that the one-dimensional calculation performed here is adequate.

I. INTRODUCTION

The interaction of an exciton or an electron with lattice vibrations leads to a number of interesting effects.[1–3] If the exciton-phonon interaction is weak, the major effects are a reduction in mobility due to scattering, the introduction of phonon sidebands in optical absorption,[4–6] a small change in mass, etc. For very strong coupling the phenomenon of self-trapping[7,8] occurs. Here, the distortion of the lattice in the vicinity of the exciton leads to a large increase in effective mass. At high temperatures, the motion of the particle through the lattice changes from band type to activated hopping.[9]

This paper is concerned with the transition be-